GA–A26067

PLASMA INITIATION AND STARTUP STUDIES IN THE DIII-D TOKAMAK WITH SECOND HARMONIC ELECTRON CYCLOTRON ASSIST

by
G.L. JACKSON, M.E. AUSTIN, J.S. deGRASSIE, A.W. HYATT,
J.M. LOHR, T.C. LUCE, R. PRATER, AND W.P. WEST

JUNE 2008

GENERAL ATOMICS

DISCLAIMER

GA–A26067

PLASMA INITIATION AND STARTUP STUDIES IN THE DIII-D TOKAMAK WITH SECOND HARMONIC ELECTRON CYCLOTRON ASSIST

by
G.L. JACKSON, M.E. AUSTIN, J.S. deGRASSIE, A.W. HYATT,
J.M. LOHR, T.C. LUCE, R. PRATER, AND W.P. WEST

This is a preprint of an invited paper to be presented at the 15th Joint Workshop on Electron Cyclotron Emission and Electron Cyclotron Resonance Heating to be held in Yosemite National Park, California on March 10–13, 2008 and to be published in the Proceedings.

Work supported by
the U.S. Department of Energy
under DE-FC02-04ER54698

GENERAL ATOMICS PROJECT 30200
JUNE 2008

GENERAL ATOMICS

ABSTRACT

Second harmonic X-mode (X2) electron cyclotron (EC) heating has been used in DIII-D to examine plasma initiation and burnthrough of low Z impurities. Although the toroidal inductive electric field (E_ϕ) in DIII-D is high enough (0.9–1.0 V/m) to allow robust startup without EC assist, startup in fusion devices such as ITER will have lower fields (E_ϕ = 0.3 V/m) and EC assist can provide an increased margin for burnthrough of low Z impurities. ECH, applied before the inductive electric field, is used to separate the various phases of plasma breakdown and startup. Ionization first occurs near the X2 resonance location and then expands in the vessel volume. Perpendicular launch ($k_\parallel$ = 0) is required for X2 pre-breakdown, and the power threshold can be reduced by optimizing prefill and vertical field, although the lowest power threshold is not at the optimum value for *Ohmic* startup. An orbit following code confirms that cold electrons (0.03 eV) can be sufficiently heated by ECH to energies above the threshold of ionization of hydrogen. This code predicts successful ionization in future tokamaks such as KSTAR and ITER. The ITER startup scenario has been simulated in DIII-D experiments and X2 ECH assist has been applied at reduced toroidal loop voltage to assist burnthrough and plasma current ramp up.

1. INTRODUCTION

Second harmonic X-mode (X2) electron cyclotron (EC) heating has been used in DIII-D to examine plasma initiation and burnthrough of low Z impurities. Although the toroidal inductive electric field (E_ϕ) in DIII-D is high enough (0.9–1.0 V/m) to allow robust startup without EC assist, startup in fusion devices such as ITER will have lower fields (E_ϕ = 0.3 V/m) and EC assist can provide an increased margin for burnthrough of low Z impurities.

Second harmonic X-mode EC assist was demonstrated in early tokamak experiments (circa early 1980s) and more recently on JT-60U, T-10 and DIII-D. In this paper, we will present recent EC-assisted startup studies in DIII-D.

The DIII-D EC system consists of six 110 GHz gyrotrons each with a nominal output power of 1 MW at the tube. The gyrotron power is routed by circular waveguides (HE_{11}) to steerable mirrors that inject the EC power into the tokamak from the low field side (LFS). Both X-mode and O-mode polarizations are possible with this system and both the poloidal and toroidal injection angles can be changed between discharges (future upgrades will allow position changes during a discharge). A previous 60 GHz ECH system was also used in DIII-D and results from LFS X2 EC-assisted breakdown with this system from experiments in 1987 are consistent with the present work.

An example of EC assisted plasma startup is shown in Fig. 1 and is compared to the normal DIII-D Ohmic case. In this paper, plasma startup is divided into five phases: collisionless heating, avalanche, plasma expansion, burnthrough, and rampup. The first three phases are generally referred to as breakdown and require an external heating source: either ECH or Ohmic in DIII-D. In Ohmically heated discharges, these phases can overlap. In the present work, in order to study the effect of EC in each phase, the ECH is applied well before the application of the toroidal inductive voltage, V_{loop}. An example of this in DIII-D is shown in Fig. 2 where plasma breakdown, i.e., the ionization, avalanche, and plasma expansion phases, all occur while V_{loop} is zero. In the first phase (collisionless heating), as the EC power is increasing, electrons are heated to energies where ionization occurs [1]. This phase is followed by an avalanche phase where the number of charged particles (ions and electrons) increase exponentially. With Ohmic heating this phase can be described by the Townsend avalanche [2] and similar temporal behavior is noted with ECH in the absence of an applied toroidal electric field, E_ϕ, although the physical mechanisms are different. The avalanche phase is followed by a plasma expansion phase where the discharge expands to fill a large fraction of the vessel volume. These phases are usually referred to collectively as plasma breakdown, and in Fig. 1, with ECH, all occur during the time before any inductive voltage is applied. After breakdown, a current channel forms and the discharge is heated. During this phase, line radiation, usually from low Z impurities such as oxygen and carbon, must be lower than the input power in order for the discharge to successfully

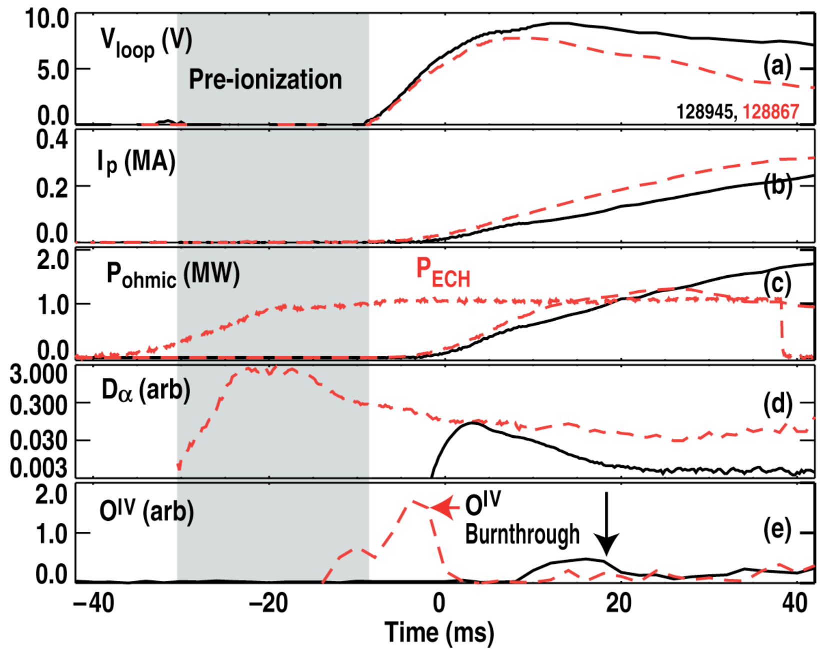

Fig. 1. Comparison of Ohmic (solid lines) and EC-assisted (dashed lines) startup in DIII-D. Plotted are: (a) inductive loop voltage, (b) plasma current measured by a poloidal array of magnetic probes inside the vessel, (c) Ohmic and EC heating power, (d) D_α line radiation, and (e) oxygen line radiation, O^{IV}, measured by the SPRED UV spectrometer.

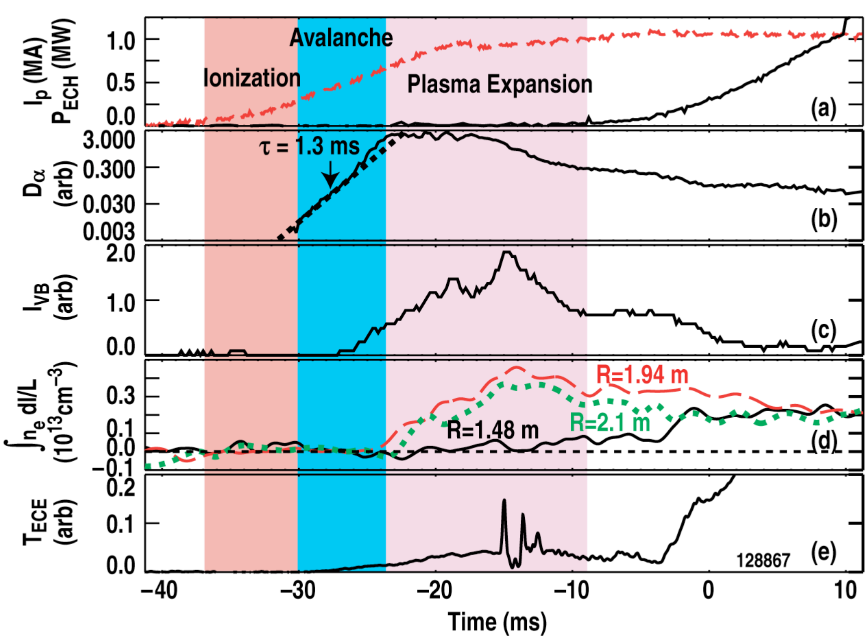

Fig. 2. Three phases during breakdown: collisionless heating, avalanche, and plasma expansion. Plotted are: (a) ECH power and plasma current, (b) D_α line radiation (note log scale), (c) visible Bremsstrahlung emission channel closest to the EC resonance location (R_{X2} = 1.85 m), (d) line integrated density from three interferometer chords, and (e) ECE emission, f=108.5 GHz.

evolve to the current ramp up phase. When the plasma electron temperature is sufficiently high, typically $\geq$ 100 eV, these low Z impurities are ‘burned through’, i.e., the impurity ion’s line radiation is no longer a dominant contributor to the total radiation. In the usual case, as the plasma’s electron temperature is temporally increasing, the line intensity of successively higher charge states first increases and then is ‘burned through’. An example of the burnthrough of one impurity charge state, O^{IV} line radiation, during this process is shown in Fig. 1(e). We note in this example, that higher charge states of oxygen (at higher T_e) must also go through this process before the plasma achieves complete burnthrough. In Fig. 1(e), O^{IV} burnthrough occurs earlier, and at lower I_p when ECH is applied. The final phase of plasma startup is rampup, where plasma current increases and edge safety factor (q_{95}) decrease to their flattop values. EC heating can effectively assist in all these phases.

A 16 channel visible Bremsstrahlung (VB) array is used to determine where ionization initially occurs. The VB-measured intensity can be written.

$$I_{VB} = \int_L c_1\, Z_{eff}\, n_e^2 / \mathrm{sqrt}\,(T_e)\, d\ell \tag{1}$$

where Z_{eff} is the effective ion charge, n_e is the electron density, and T_e is the electron temperature integrated along the viewing chord line of sight.

For this work, we will show the VB intensity from each channel, as a function of its radius of tangency in the discharge. Density is measured with three interferometers whose vertical paths are at different radii. D_α emission was obtained with two arrays of visible photodiodes. A UV spectrometer viewing radially from the midplane was available to measure impurity line radiation.

2. BREAKDOWN IN DIII-D WITH ECH

With ECH the first three phases, collisionless heating, avalanche, and plasma expansion, occur before the onset of the inductive electric field, and thus can be studied separately. An example is shown in Fig. 2. In this case, the EC power is ramped up slowly to determine a power threshold. Once ionization occurs, defined by the first occurrence of either D_α line radiation or VB intensity, the intensity of the D_α light increases exponentially over more than 1 order of magnitude [Fig. 2(b)]. If we assume that this intensity is proportional to deuteron density [3], then the avalanche process with ECH has a form similar to the Townsend avalanche [4].

Near the end of the avalanche phase, electron density begins increasing in the two IR interferometer chords, Fig. 2(d), whose radii are located outboard of the EC X2 resonance radius. This is the start of the plasma expansion phase. However the density detected inboard of R_{X2} remains low until the onset of plasma current. We also note that bursts of ECE emission are observed during the plasma expansion phase, Fig. 2(e). The physical mechanisms for the ECE emission are not understood and will require further investigation.

The VB array has been used to identify the ionization location by observing the chord with the highest initial intensity. Plotted in Fig. 3 are profiles at various times, from first detection through the plasma expansion phase. As discussed in Section 1, VB emission is plotted as a function of radius of tangency of each chord. Contributions to inner channels, which pass through the region of maximum intensity, are higher than for an Abel inversion that would calculate the emission at a given radius. Nevertheless, this analysis shows that maximum intensity occurs for the VB channel near, but inside, the X2 resonance location. Note that during the plasma expansion phase (t = –10 ms in Fig. 3) the profile broadens. The decrease in total intensity is due to increasing electron temperature [Eq. (1)]. The resonance location was varied from near the inner wall to beyond the vessel center (R_0 = 1.67 m), 1.13 m ≤ R_{X2} ≤ 1.83 m by changing the toroidal field. The radius of initial ionization occurs near, or at, the X2 resonance location in all cases.

A series of scans and comparisons have been performed to determine the conditions for EC ionization. Theory predicts that LFS 2nd harmonic O-mode (O2) heating efficiency is very low [5], and would not be expected to provide ionization with the ECH power used in this work. As predicted, no breakdown is observed for a discharge with O2 heating before E_ϕ is applied when compared with a discharge using X2 ECH under similar conditions where breakdown is observed. A toroidal angle scan is plotted in Fig. 4 showing that the strongest ionization occurs when $k_{||} = 0$, i.e., when the launch angle is perpendicular to the toroidal field.

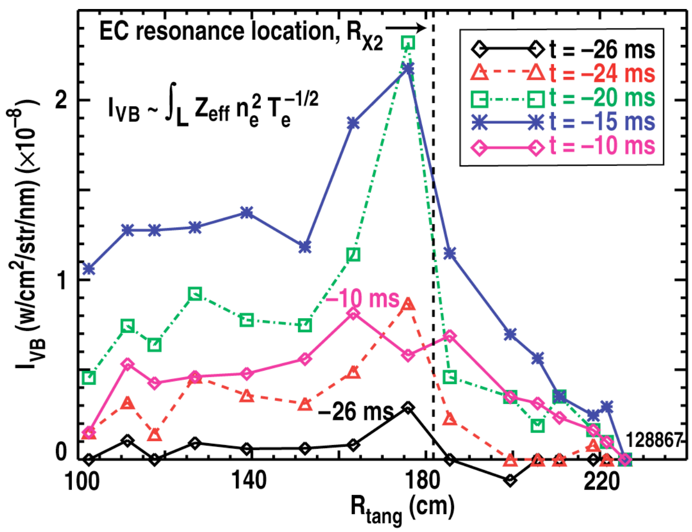

Fig. 3. VB emission profiles at times during the avalanche and plasma expansion phases, defined in Fig. 2.

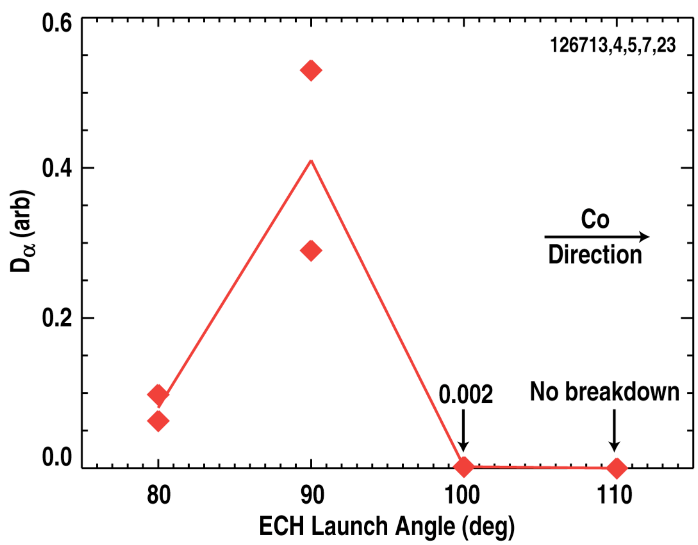

Fig. 4. EC angle scan. A launch angle of 90 deg corresponds to perpendicular injection ($k_\parallel = 0$). Parameters are: $P_{ECH} = 1.3$ MW (110 GHz) and $R_{X2} = 1.51$ m.

An important consideration for DIII-D and future tokamaks is the power level at which EC ionization can occur. Initial results using the old 60 GHz system showed a power threshold of 0.38 MW, of which 0.25 MW was X2 polarization. This was done at fixed parameters. However, recent experiments with the 110 GHz system showed that the power threshold varies by more than a factor of 3 and is sensitive to both neutral deuterium prefill pressure and vertical magnetic field, B_{VF}. An example of a vertical field scan is shown in Fig. 5, where the most robust EC ionization occurs at the highest B_{VF}. This result is counter-intuitive since a larger vertical field represents a lower connection length for an ionizing electron from the EC resonance location to the wall. In general a longer connection length would imply an electron has a higher probability of ionizing collisions with neutral deuterium. For the three cases in Fig. 5, the connection length from the EC heating region to the wall of 0, 20, and 40 G are 0.5, 0.82, and 0.33 km, respectively. This result will be discussed further in Section 5.

Although not plotted, the range of neutral prefill pressure is also larger with ECH. In fact, the most robust breakdown occurs at higher prefill pressures than are normally used for Ohmic startup.

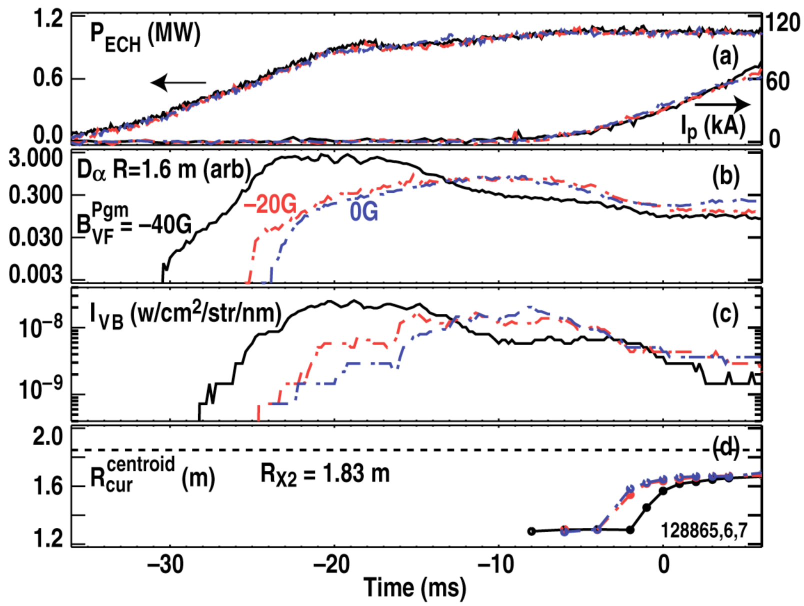

Fig. 5. ECH power threshold, (a) for three values of applied vertical field: 0 G (dash-dot), –20 G (dash) and –40 G (solid). D_α line radiation is plotted logarithmically in (b), VB intensity is shown in (c), and the plasma current position using a single filament fit is plotted in (d).

3. COLLISIONLESS HEATING

In the collisionless heating phase (Fig. 2), electrons are heated until there are sufficient ionizing collisions to sustain an avalanche [4]. An electron energy, W_e, of at least 20 eV is required to ionize hydrogen [1]. This phase was modeled with an orbit following code [4]. In this model, an electron is assumed to have an isotropic thermal velocity and heating occurs as it drifts through the EC beam. Perpendicular heating is assumed ($k_{\parallel} = 0$) so the parallel drift velocity is constant. During the collionsless heating and avalanche phases plasma density is very low, so the electrons only suffer collisions with neutrals. The effective electron-neutral collision length is long, estimated to be 3.7 m in Ref. [4] for typical DIII-D parameters, so electrons do not lose coherency, and they are effectively heated over many orbits. This heating has been modeled with an orbit following code. An example is plotted in Fig. 6 using the geometry from the previous 60 GHz DIII-D ECH system. In this example, the model predicts that a cold seed electron (0.03 eV) can be heated to 35 eV, above the threshold for ionization. Also shown in Fig. 6 is the electron drift length (L_z) in the parallel direction to B. Since this parallel electron drift is less than the EC beam diameter and since the total distance an electron traverses along its orbit (L_{heat}) is less than the effective electron-neutral collision length, 3.7 m, the model predicts collisionless electron heating to energies above the ionization threshold. Note that this model also includes relativistic effects as the electron is heated, which tend to decorrelate the heating and limits the maximum achievable temperature range. The initial heating from this model also agrees closely with the analytic expression derived from Ref. [4] and is plotted in Fig. 6.

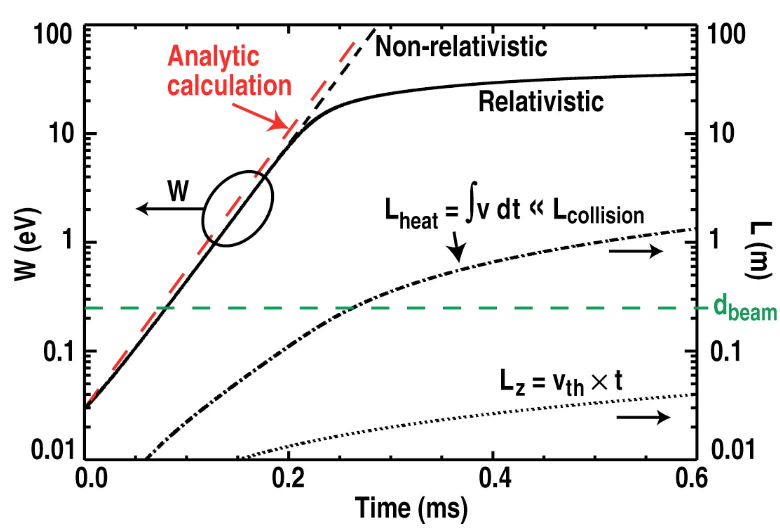

Fig. 6. Heating results from the orbit following code for a 60 GHz case with T(0)= 0.03eV, P_{X2} = 0.15 MW, and d_{beam} = 0.24 m.

4. EC STARTUP IN FUTURE TOKAMAKS AND DIII-D SIMULATION EXPERIMENTS

A key question is whether EC assist will be effective in future tokamaks such as ITER and KSTAR where thick liners and superconducting coils limit the maximum inductive electric field (E_ϕ). In ITER, this limit is $E_\phi \leq 0.3$ V/m and EC assisted startup is planned to provide an additional margin. Although both ITER and KSTAR have planned for fundamental ECH during startup, it may be necessary in certain scenarios (e.g., commissioning) to have EC assist at reduced toroidal field and X2 EC startup may be needed. Using the collisionless model described in Section 3, we predict that X2 ECH can heat low energy (0.03 eV) seed electrons to energies above the ionization threshold in both ITER and KSTAR.

After breakdown, burnthrough and current ramp-up (Section 1) must occur for successful discharge initiation. During these phases, the discharge shape evolves. In order for ECH to be effective, the resonance must be inside the last closed flux surface. In the baseline ITER scenario the discharge starts as a small volume limited on the LFS and increases at constant q_{95}. Because of this, the main 170 GHz ECH resonance is not within the plasma volume during the critical early burnthrough phase, and an additional 3 MW 127 GHz gyrotron system has been specified for ITER to heat this small volume plasma. DIII-D experiments simulating the ITER baseline scenario showed that the value of ℓ_i did not meet the ITER constraints [6]. In addition, limiter heating in ITER during this LFS limiter phase would be near the engineering limits. Hence an alternate scenario has been developed and tested in DIII-D consisting of a larger initial plasma volume, referred to as the ‘large bore’ scenario, and diverts earlier to reduce LFS limiter heat flux. DIII-D discharges with the large bore scenario are shown in Fig. 7. Since the X2 resonance is inside the plasma volume during the burnthrough phase, EC heating effectiveness in the ITER shape can be evaluated. One example is shown in Fig. 7(f), where burnthrough of the O^V line radiation occurs earlier with EC heating. We note that O^V burnthrough is only an example of the burnthrough phase: burnthrough of the higher oxygen charge states is also required. Also shown in Fig. 7 is the effect of reducing V_{loop} and, hence, P_{Ohmic}. With lower Ohmic heating power O^V burnthrough occurs later than the higher voltage case. However with ECH, this burnthrough is prompt, occurring even faster than in the higher voltage case. This additional input power to assist burnthrough may allow a more robust startup in ITER. In addition to improved burnthrough with EC assist, the V-Sec consumption (at the same I_p) is reduced when comparing the low voltage startup with and without ECH (Fig. 7). However, as discussed in Ref. [2], the V-sec improvement in primarily limited to the burnthrough phase. Note that for the large-bore scenario, burnthrough occurs with both the 127 GHz and 170 GHz resonances inside the plasma volume. This would allow higher power and the flexibility to operate at reduced toroidal field if both ECH systems were used during startup.

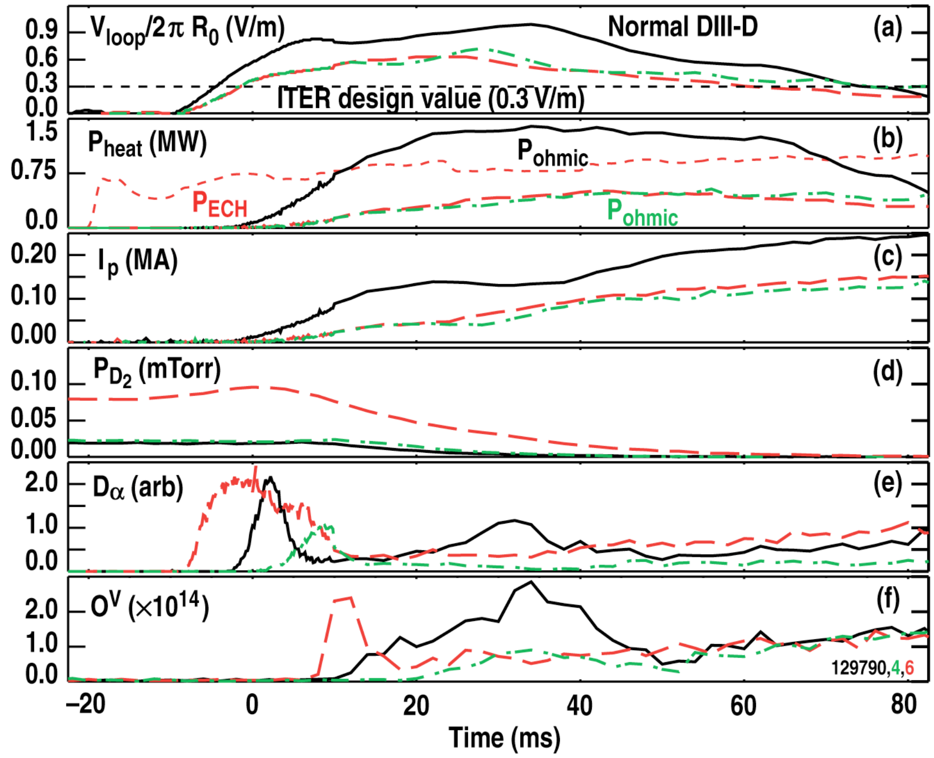

Fig. 7. Startup for ITER-like large bore discharges with reduced V_{loop} (dash and dash-dot) compared to the normal voltage for DIII-D startup (solid). The reduced voltage discharge with ECH (dash) shows the earliest ionization (e) and burnthrough of O^V line radiation (f). Also shown are: (b) P_{Ohmic}, (c) plasma current, and (d) neutral pre-fill pressure.

SUMMARY

Second harmonic X-mode EC breakdown in DIII-D is robust and reproducible. It is most effective with perpendicular launch and, in fact, is barely detectable for launch angles ≥ 10 deg from perpendicular. We note in passing that results on T-10 show breakdown over a wider range of launch angles [7]. The reasons for this discrepancy between T-10 and DIII-D have not been resolved. As predicted by theory, no breakdown was observed using O2 ECH before the inductive voltage was applied. With X2 ECH, the initial ionization and avalanche initially occurred near the resonance radius and then broadened later in time. This was observed as the X2 resonance location was scanned from 1.13 m < R_{X2} < 1.83 m and was consistent for both previous 60 GHz and 110 GHz results. During the plasma expansion phase, the density detected by IR interferometers was primarily outboard of R_{X2}. Although the VB array did not show this in/out asymmetry, we speculate that the more accurate Abel inversion of the VB profile data would be consistent with the density data and would indicate even more peaking of the VB profile near the X2 resonant radius at earlier times during the avalanche phase.

The ECH power threshold was reduced a factor of 3 by increasing the prefill neutral pressure and applying a 40 G vertical field. One reason that this vertical field allowed breakdown at the lowest power threshold may be that the flux surface in the –40 G case is better aligned with the resonance radius. Hence multi-pass absorption would be more effective in heating cold electrons. Additional modeling is required to confirm this hypothesis. Nevertheless, it is clear that by a careful choice of B_{VF}, and possibly alignment of the electron's drift trajectory to the wall, the power threshold for breakdown can be significantly reduced. We also note that these EC startup experiments in DIII-D were designed to separate the various phases of the startup scenario. In actual operation, these phases would overlap and, in fact, ECH would probably be applied coincident with the initiation of the inductive electric field in ITER.

A collisionless heating model has been developed that predicts cold electrons (0.03 eV) can be heated to temperatures above the ionization threshold of 20 eV for both the DIII-D 60 GHz and 110 GHz systems, consistent with experimental observations. This model has been applied to both KSTAR and ITER, using their design parameters. It is predicted that their ECH systems can also heat cold electrons to values well above the ionization threshold: a necessary condition for EC ionization in these devices. The use of ECH may relax the constraints on field errors for these devices, since ECH can provide effective burnthrough and startup assist. The ITER startup scenario has been simulated in the DIII-D tokamak. In the original scenario, the internal inductance was higher than required for ITER so an alternate scheme was developed that also reduced heat flux to the LFS limiters by diverting earlier. The application of ECH to this scenario allowed an earlier ionization, nearly coincident with start of inductive voltage and also a faster burnthrough of low Z impurities.

It is important to note that optimum conditions for EC-assisted breakdown, burnthrough, and startup may differ significantly from Ohmic conditions. An applied vertical field actually improved the EC-assisted breakdown and pre-fill pressures higher than normally used for Ohmic plasmas also seem to improve the EC-assisted breakdown and burnthrough phases. Breakdown with higher error fields, as demonstrated by the vertical field scan, may allow an additional degree of freedom when designing future tokamaks, i.e., error field requirements (and power supply constraints) may not be as stringent if EC assist is used.

REFERENCES

[1] A. von Engel, *Ionized Gases* (Oxford: Clarendon, 1955).

[2] B. Lloyd *et al*. *Nucl*. *Fusion* **31**, 2031 (1991).

[3] L. C. Johnson and E. Hinnov, *J*. *Qunt*. *Spectros*. *Radiat*. *Transfer* **13**, 333 (1973).

[4] G. L. Jackson *et al*. *Nucl*. *Fusion* **47**, 257 (2007).

[5] R. Prater *Phys*. *Plasmas* **11,** 2349 (2004).

[6] G. L. Jackson *et al*. ITER startup studies in the DIII-D tokamak, submitted to *Nucl*. *Fusion* (2008).

[7] N. A. Kirneva *et al*. *Proc*. *34th European Conf. on Plasma Physics, Warsaw, Poland, 2007* (Europhysics Conference Abstracts 2007) Vol. 31F, P1.164.

ACKNOWLEDGMENT

This work supported by the U.S. Department of Energy under DE-FC02-04ER54698.